Automated Fiber Placement Path Planning: A state-of-the-art review

Guillaume Rousseau[1] (ID) , Roudy Wehbe[2] (ID) , Joshua Halbritter[3] (ID) and Ramy Harik[4] (ID)

[1]McNair Center, University of South Carolina, guillaume.rousseau@phelma.grenoble-inp.fr
[2]McNair Center, University of South Carolina, RWEHBE@email.sc.edu
[3]McNair Center, University of South Carolina, halbritj@email.sc.edu
[4]McNair Center, University of South Carolina, HARIK@mailbox.sc.edu

ABSTRACT

Design and manufacturing of composite structures are driving the next generation innovation cycles for the aerospace, automotive and energy markets. Automated fiber placement (AFP) is quickly becoming the preferred manufacturing method of those structures as it offers manufacturing automation, reduces production cycle times, and decreases human induced errors. One of the major steps towards manufacturing structures with AFP technology is the selection of the optimal layup strategy. This is limited by, not only geometrical and process parameters, but certification allowable and guidelines. This paper outlines a systematic review of the multiple layup strategies practices currently used and/or investigated for the AFP manufacturing process. The optimal layup strategy needs to be selected and verified to obtain laminates with little to no manufacturing defects. Through a methodical description, the different layup strategies found in the literature are described as well as their mathematical implementation. Following, a geometrical benchmark is presented so that new layup strategies can be compared to others based on the same reference. The article can be the foundation for any new layup strategy investigation.

1 INTRODUCTION

The first Automated Fiber Placement (AFP) machines (such as the one presented in the patent [67]) were developed in the beginning of the 1980's and then commercialized in the 1990's. Their development was possible thanks to aerospace industries, because of the need to improve the composites additive layup process. Indeed, composites are becoming more commonplace because of their competitive strength to weight and stiffness to weight ratio. In
Figure 1, the tendency of an increase in the use of composites of the aircraft industry is illustrated. Indeed, advanced aircraft structures such as Boeing 787 and Airbus A350 XWB contain about 50% by weight of composite components [44].
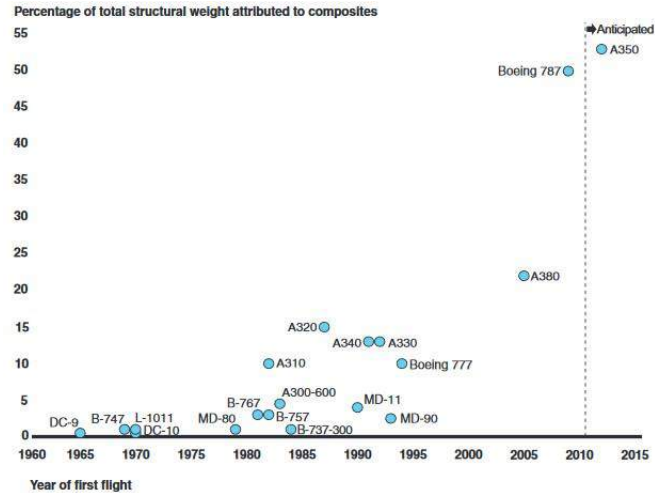
Figure 1: Different planes with their percentage by weight of composite [65].

Creating a large composite part requires the placement of several stacked plies, which are composed of many courses that contain the individual parallel tows of fiber material. To move from one course to the other, a motion system such as a robotic or a gantry one is used. The different plies can have different orientations. The most common ones are 0°, 90°, 45° and 135° (-45°). These angles apply to the actual orientation of the fibers, which control the mechanical properties of the ply. Plies of different orientations can also be superposed to have the desired composite properties on the surface. This is why the most common angles are those cited previously as they provide a quasi-isotropic structure easier to predict, analyze and certify.

In order to layup these plies properly, one needs to program the different paths of the machine. Indeed, starting with planar surface, it is easy to pursue how to lay the different plies with the proper fiber angles. However, as it will be shown in this paper, the AFP process is not only limited to 2D surfaces. This is why, many layup strategies for AFP manufacturing exists in order to cover different type of surfaces. This paper is a review of the different layup strategies which exist for automated fiber placement.

Section 2 provides a description of the AFP process focusing on the different parts of the AFP machines head and their functions. Section 3 covers the layup strategy conditions that define the general placement of the fiber tows. Additionally, it covers the common defects that will be imparted to the layup during manufacturing that may result either from a chosen layup strategy or process related errors. Sections 4 covers the common layup strategies and how they define a reference curve. These primary reference curves will be constant curvature paths, geodesic paths, constant angle paths and variable angle paths. Finally section 5 discusses the coverage strategies and how they propagate from reference curves in order to achieve full ply coverage within the defined ply boundaries.

2   DESCRIPTION OF THE AFP PROCESS

In this section, a description of the AFP process needed to understand the layup strategies is presented. First, the basic terminology of the AFP process are defined. Following, the different functions of the AFP machine head are detailed.

2.1 Terminology

The purpose of this subsection is to familiarize the reader with the different basic terms of the AFP process.

- Tool: The preform which defines the shape for the layup process. It provides the base geometry for applying consecutive layers (these layers are named plies) of material in order to build up the desired part (called a laminate). The numerical model of this will be used to generate the machine motion numerically and potentially used for simulation of the layup process before real world usage.
- Laminate: A laminate is a group of plies
- Ply: A grouping of courses that exist in the same layer of a part. By laying up several plies of thin material, one is able to achieve the desired thickness of a part.
- Course: A combination of several parallel tow-paths which traverses a parts geometry, feeding material from one or more rolls of material. A course can be composed of 6 to 32 tows (typical AFP machines). If several material feeds are utilized, each may be individually started and cut to achieve near net layups. Courses may be linear or steered, in addition to rotation of the head, to achieve the desired strength characteristics of the final part.
- Tow: A narrow strip of continuous carbon fiber, generally 3.2 mm up to 12.7 mm wide (respectively 1/8 and 1/2 inches). Due to the reduced width, many tows may be fed from an automated fiber placement machine to achieve higher surface coverage per course. Typically, the fiber will be pre-impregnated with either a thermoset or a thermoplastic, or may even be dry fiber which will use a resin infusion process to generate the final composite matrix afterwards.

2.2 Description of the AFP process

The AFP machine is divided in three parts which carry different functions during the AFP process. The first part allows the motion of the machine, the second part is the machine head which handles the layup process [41], and the last part is the tool support. In this section, the different part of the AFP machine head (
Figure 2) are detailed. These functions are feeding the head with the tows (2.2.1), cutting the tows (2.2.2), heating the tows (2.2.3) and compacting them on the tool surface (2.2.4). In section, all this function will be described.
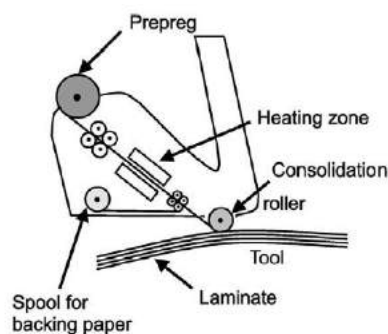
Figure 2: Fiber placement head diagram [18].

2.2.1 Tape feed

Tape feed unit is composed of directional rollers which allow independent tows to arrive at the top of the fiber placement head with a good tension. Depending on the type of machine being used, the

tape feed unit can deliver up to 32 independent tows to the fiber placement head. As every tows are independent, for complex surfaces with high steering, the courses feed can be different to minimize the defects. Often times, measure of this feeding mechanism is used to confirm the accuracy of as design and manufactured.

2.2.2   Cutting unit

The control of cutting as well as the machine's cutting tool need to be very precise, as there is always need to improve AFP processes and layup tows more rapidly [17]. As the name suggests, the cutting unit needs to cut the tows at the right time to have the needed layup. This elevates the precision and the accuracy of the final composite structure.

2.2.3   Heat source

Many heat sources can be installed on the fiber placement head [21],[76], the most common ones are infra-red (IR) heater, hot roller, hot gas heater. Laser heaters, hot rollers, and hot gas heater are used for thermoplastic fibers deposition. Indeed, they are more effective and more precise as they can heat the tows rapidly but they are much more expensive than the other techniques. A new technology has been recently developed and is called the humm3™ [31]. This new heating source is a flash lamp and can be used for thermoset, thermoplastic and dry fiber composites. It has the same power as a laser but is more precise as the operator can control the energy, the duration, and the frequency of each pulse. Its small agile head placed on an automated fiber placement head allows the deposition of composite on complex surface. Another function filled by the heat source is to flash the tows before starting to lay the course on the surface or the previous ply. The flashing procedure ensures that the temperature of the surface and new tows is high enough to guarantee proper tacking.

2.2.4   Consolidation or compaction roller

The compaction roller is used to press the tows onto the tool surface or the previous ply. It eliminates entrapped air and inner gaps [41]. It enables the tows to adhere quickly and remain in place.

3   PREAMBLE

In this section, three different conditions for the courses trajectory to be validated are described. Of course, these conditions change with the structure and the mechanical properties one desires for the final composite part.

3.1   Direction of the fiber

The different courses laid up by the AFP process need to be placed in a way that the fibers orientations respect the required specifications. Indeed, most of the time, it is asked to make plies with fibers having a well-defined angle as 0°, 90°, 45°, -45° [59] as they provide a quasi-isotropic behavior for the structure. The 0° angle direction can follow the longest dimensions of the surface as in
Figure 3. It is simple to lay up plies with these angles on a flat panel (
Figure 3) however on complex surfaces, it is more difficult as the fiber angles in the tow can change due to the geometry of the surface. This is why many different layup strategies appeared as one cannot use the same strategy to obtain the same structure as the tooling surface changes. This paper details all the layup strategies found in the literature for the AFP process to be able to choose the right strategy on the proper tooling surface to obtain the wanted structure.

3.2   Minimum turning radius

Another condition to check before finalizing the path design is the turning radius or the curvature of the path. Since the tows used in the AFP process have a finite width, the edges of the tow will be either under tension or compression while trying to adhere a rectangular shaped tow on a curved

path. This mismatch in length between the tow and the actual path on the surface will push the excess material to buckle out-of-plane to form a wrinkle (
Figure 4) on the compressive edge of the tow. As for the tensile side, the shortage of material will push the fibers to move closer to the center line leading to tow straightening, or in the severe cases to move out-of-plane and fold over ([70],[71]).

To avoid these defects (see section 3.3.3), a minimum steering radius has to be set beforehand depending on the material to be used. Usually, the minimum steering radius is determined experimentally by trying different radii of curvature with different combination of process parameters (speed, temperature, roller pressure).

a) 90°

b) 0°

c) 45°

d) -45°
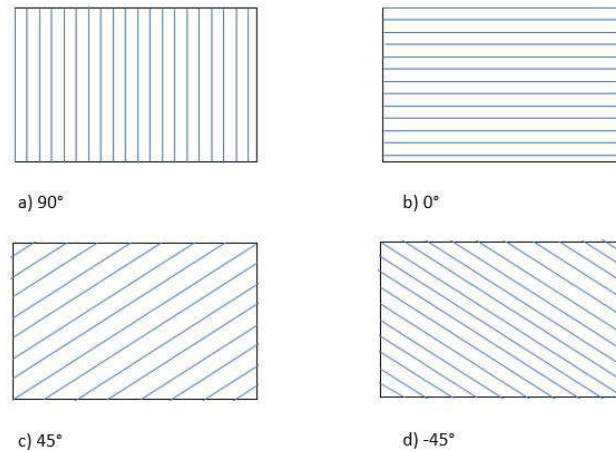
Figure 3: Flat panel with different layup fiber angles.

Tow misalignment

Tow buckling

Tow pull up
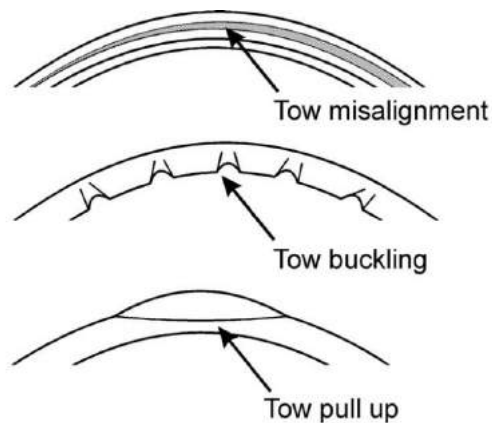
Figure 4: Most common tow steering defect [18].

3.3 Common Defects

Due to material stiffness of carbon fiber tows, an optimal layup strategy should be chosen which reduces the occurrence of defects. The defects that can be encountered during the AFP process [27] are summarized in Tab.1.

Defects	Definitions
Gaps/Overlaps	Gaps or overlaps can occur between two tows or two courses. A gap will weaken the structure while an overlap will increase its weight.
Wrinkle	A wrinkle is a short section of fiber that has raised off the tool due to excess heat or excessive steering. In these cases, the fiber has failed to fully adhere to the previous layers and create an uneven surface.
Bridging	Bridging appears very similar to wrinkling, and describes the failure of fiber paths to adhere to the tool surface. The tensions of the tows overcome the tows' adhesion to the surface, inducing the bridging. This is typically found with ply drops.
Twisted Tow	The tow has rotated on itself before being placed on the surface by the compaction roller.
Splice	A splice is when a tow ends and the next tow is superposed to the previous one during many inches.
Missing Tow	When a tow is not laid on the surface or does not adhere on it. This defect can be linked to an issue during the feeding function.
Foreign Objects or Debris	An object or a debris are laid under or on a tow. This will have an impact on all the following plies.
Fold/Roping	When the feeding system does not deliver the tow with the right orientation or the right tension, the laid tow will have a cylindrical shape more than a planar one on the surface.
Position Error	A tow placed on the wrong location.
Loose Tow	A loose tow is a tow which does not fully adheres to the previous ply. This is typically link to heat or compaction issues.

Table 1: Definitions of the defects encountered during the AFP process [27].

4   REFERENCE CURVES

Before covering the surface, an initial (or reference) curve is needed. In this section, the different strategies to find the reference curve will be detailed. Either parametrical approaches, or the use of a mesh, can be found in the literature. Both methods have advantages and drawbacks which have been summed up by [13] for automated spray painting. A mesh provides useful information, such as the different areas of the facets and their normal, which are important to generate the toolpath along the course. Nevertheless, a mesh is an approximation of the surface so the precision obtained depends on how accurate the mesh is. One can keep in mind that a more refined mesh would increase the computation time. Using a parametrical approach, the surface would be known more precisely. In this section and the following ones, we will detail different strategies to find reference curves.

4.1   Fix angle reference curve

Using a fix angle strategy, the fiber angle in the reference curve is constant all along the surface. This layup strategy is a very used as it allows a complete control of the fiber angles along the surface. A first approach of a constant angle reference curve calculated using a mesh is given, then the way of finding the reference curve using a parametrical approach will be developed.

4.1.1   Using a mesh

The method presented in [48] uses the mesh information contained in a STL file. After a preliminary computation to perform initial topology reconstruction a functional model including the vectors/edges, the nodes, the facets, and the normal vectors of the facets is generated. If one uses another mesh file type, these information need to be first generated to enable the usage of this method. For instance, to find the normal vectors from the vertices of a triangular mesh a method is

provided in [39]. Using these information, a first slicing algorithm is used to create the reference curve. Basically, a tangent plane in one direction is used to find all the points on the mesh which intersect this plane (
Figure 5). To do so, a first point, P_1, of a triangle which intersects the plane and the edge is found. Then, thanks to the structure reconstruction, the mesh triangle in which this point belong is already known. Finally, the second point, P_2, of the triangle mesh intersecting the plan is found and we can move forward to the next triangle this last point belongs to. This loop is made until the tangent plane does not intersect the surface anymore. The fact that the direction of the tangent plane used is constant makes the fiber angle constant along the surface.
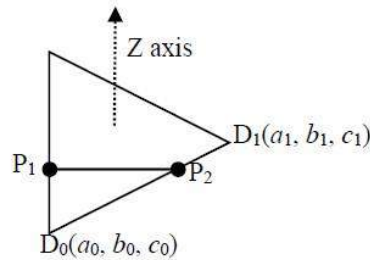
Figure 5: Fix angle reference curve using a mesh [48].

To find another fix angle path, the meshed plane is rotated by a constant angle from the previous path defined before. In
Figure 6, the rotation around the z-axis of the triangle $D_0D_1D_2$ by an angle of 45° gives a new triangle $D_{00}D_{11}D_{22}$. In this diagram, the reference curve is v and P_0P_1 is the offset of this reference curve at a fixed angle of 45°.
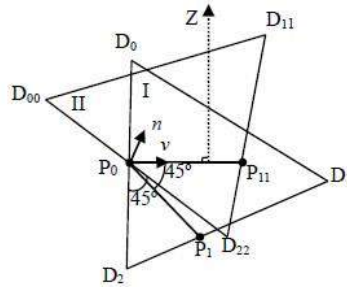
Figure 6: Constant angle method [48].

4.1.2 Parametrical approach

As said before, the parametrical approach is more dominant in the literature.
In [20],[45],[58],[60],[69],[77] a major axis is projected on the surface S(u,v) = [x(u,v), y(u,v), z(u,v)]. This projection gives an intersection line on the surface. The major axis plane equation is P(x,y,z) = ax + by + cz +d = 0. Hence, the surface plane intersection equation is:

$$f(u,v) = ax(u,v) + by(u,v) + cz(u,v) + d = 0 \qquad (4.1)$$

As discrete points are needed to find the offset curves to cover the surface, points on this intersection line need to be determined. A starting point from which the reference curve will be propagated is needed. This starting point is found on a boundary using a bracket method followed by a Newton-Range method (NRM) on equation (4.1) to find the intersection point between the boundary and the

projection of the major axis. To find the next point of the reference curve, one step is done in one direction (length of the step is defined) then the other step uses the NRM to converge to the surface-plane intersection line. The propagation is done until the major axis doesn't intersect with the surface anymore (
Figure 7).

Figure 7: Projection of a major axis on the surface [60].

The same method to find the reference curve is presented in [77] but the compaction roller position is also considered. Indeed, on every point of the reference curve, a tangent plane to the surface is inserted. The center of the roller is then placed on the normal to the surface calculated in each points (Figure 8). Determining the roller path location following the reference curve allows, on very complex surfaces, to avoid defects so the laying efficiency is increased.

Figure 8: Reference curve with roller position [77].

In [28],[29], an iterative algorithm is developed using a defined reference direction. Starting from a point P_i, a tangent vector d of the surface and following the reference direction is estimated. Another vector t is created by rotating d around the normal vector by a defined placement angle φ. Finally, a point P_F is defined on this vector t at a certain distance from Pi and is projected on the surface what gives us a point P_{i+1} on the surface (Figure 9). The process is iterated until the path reaches a boundary.

Figure 9: Reference curve using an iterative algorithm [29].

Finally, [4],[7],[9] determined a reference curve for a conical shape (Figure 10). It is a good example where the parametrical approach is easier and faster than using a mesh. Indeed, it is easy to know the equation of a conical surface and deduce the equation for the fiber angles φ and the curvature κ of the reference curves. These two parameters are given in the equation below:

$$\sin \varphi(x) = \frac{r_0 \sin T_0}{r(x)} + \frac{\kappa}{\sin \alpha} \left(\frac{r(x)^2 - r_0^2}{2r(x)} \right) \tag{4.2}$$

$$\kappa = \left(\frac{r_1}{\bar{r}} \sin T_1 - \frac{r_0}{\bar{r}} \sin T_0 \right) \frac{1}{L}, \left[\bar{r} = \frac{r_0 + r_1}{2} \right] \tag{4.3}$$

Where: r_0, r_1 and α are the small, the big radii and the cone angle; $r(x)$ represents the perpendicular distance from the revolution axis to a point on the shell and varies linearly for this shell configuration: $r(x) = r_0 + x\sin\alpha$; L is the length along the surface; T_0 and T_1 are respectively the fiber orientation at the small and the big radius of the cone.
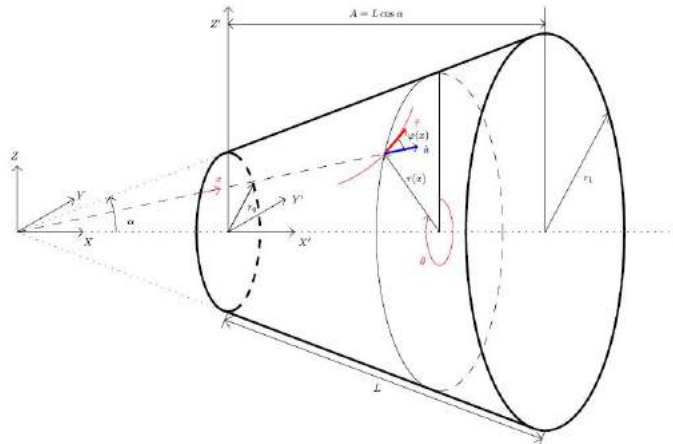
Figure 10: Cone geometry [4],[7],[9].

A resolution of equations (4.2) and (4.3) keeping the fiber angle constant gives the reference curve on the cone surface with a fixed angle.

However, as these methods only focused on the fiber angle, it is possible to have a steering too severe at some point of the reference curve what makes the manufacturing process difficult if not impossible. Indeed, on Figure 11, the constant angle path on a conical surface is represented in black

and the latter is steered on some points. This is the main reason why layup strategies need to include manufacturing configurations to generate optimal toolpaths.

(a) Paths on the 3D cone   (b) Paths on the flattened cone
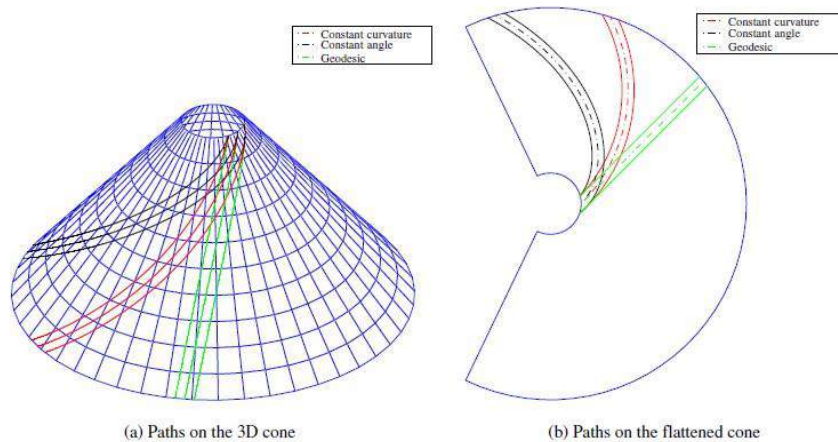
Figure 11: Constant curvature, geodesic and constant angle path on a cone (with fiber orientation of the small and the big radius equal to 45°) [4],[7],[9].

4.2 Geodesic guide curves

A layup strategy to avoid steering is to compute a geodesic guide curve. Indeed, the curvature along a geodesic path is null. An illustration of this path on a conical shape is given in Figure 11.

The geodesic path can also be known as the natural path. A geodesic is the shortest path between two points along a three-dimensional surface in Cartesian space [55]. This is why on a flat panel, the geodesic path is a straight line [25].

Also, a geodesic path can be obtained by specifying a starting point and a direction of travel. For a general parametric surface, a geodesic path has to satisfy the following system of differential equations:

$$\begin{cases} u'' + \Gamma_{11}^1 u'^2 + 2\Gamma_{12}^1 u'v' + \Gamma_{22}^1 v'^2 = 0 \\ v'' + \Gamma_{11}^2 u'^2 + 2\Gamma_{12}^2 u'v' + \Gamma_{22}^2 v'^2 = 0 \end{cases}' \tag{4.4}$$

where Γ_{jk}^i are the Christoffel symbols given in the Appendix. In order to solve this system of equations, 4 initial conditions have to be set: $u(0) = u_0, v(0) = v_0, u(1) = u_1, v(1) = v_1$ for the geodesic path between two points $P_0 = S(u_0, v_0)$ and $P_1 = S(u_1, v_1)$, or $u(0) = u_0, v(0) = v_0, u'(0) = u'_0, v'(0) = v'_0$ for the geodesic path starting at $P_0 = S(u_0, v_0)$ with a direction (u'_0, v'_0).

For the case of a flat surface, the system of equations in (4.4) can be simplified to obtain the parametric equation of a straight line which is the shortest path between two points.

In [29], a layup strategy algorithm is developed to fit a Y shape. Starting from one branch of the Y surface, and given an initial fiber angle, a geodesic path is defined. However, once at the junction of the Y, the geodesic path might change or won't be able to propagate on the surface. The different given solutions to continue the path are: to go in the direction of the minimum curvature, to try to reach a geodesic path on the other branch of the Y (Figure 12), or to create a straight path on the other branch respecting the steering conditions for the courses.
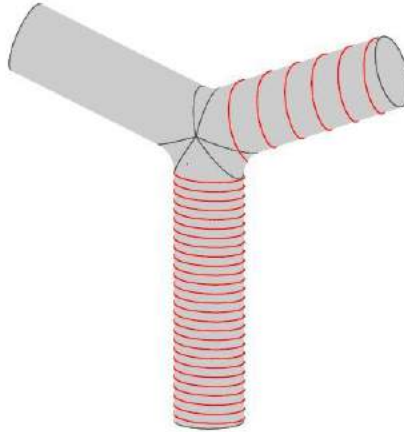
Figure 12: Reference curve on a Y surface [29].

4.3 Variable angle guide curves

The fiber orientation can vary along the reference curve. This is in contradiction with what is said in Section 3.1 as the fiber directions are not constant anymore. However, this variation of the fiber direction leads to a variable-stiffness [54],[57]. The higher degree of freedom for the reference curve allows the creation of structures which account for non-unidirectional constraints. Nevertheless, the calculations and the optimization are harder. In this section, different strategies to define the reference curve with variable angle fibers will be explained.

4.3.1 Constant curvature

For a general surface, the following system of 2nd order differential equations in terms of the surface parameters u and v has to be solved numerically with a prescribed geodesic curvature k_g, to obtain a constant curvature path:

$$\begin{cases} u'' + \Gamma_{11}^1 u'^2 + 2\Gamma_{12}^1 u'v' + \Gamma_{22}^1 v'^2 = \dfrac{k_g(F\,u' + G\,v')\sqrt{Eu'^2 + 2Fu'v' + Gv'^2}}{\sqrt{E\,G - F^2}} \\[3mm] v'' + \Gamma_{11}^2 u'^2 + 2\Gamma_{12}^2 u'v' + \Gamma_{22}^2 v'^2 = \dfrac{-k_g(E\,u' + F\,v')\sqrt{Eu'^2 + 2Fu'v' + Gv'^2}}{\sqrt{E\,G - F^2}} \end{cases} \quad (4.5)$$

In equation(4.5), E, F and G represent the first fundamental coefficients of the surface and Γ_{jk}^i are the Christoffel symbols given in the Appendix.

For a flat plate, a constant curvature path is an arc of circle, with a possible parametrization:

$$\begin{cases} x(t) = x_0 + \dfrac{1}{\kappa}\cos t \\[3mm] y(t) = y_0 + \dfrac{1}{\kappa}\sin t \end{cases} \quad (4.6)$$

where, (x_0, y_0) are the coordinates of the center, and $1/\kappa$ is the radius of curvature. Constant curvature paths are frequently used as trials to determine the critical radius at which wrinkling will occur for a given process parameters.

Another polynomial description for finding reference curves using a meshed surface with a known surface equation in the x-y system (or in a polar system) is available [29]. Assuming that the path function is: z = f(x,y), one can deduce the fiber angle θ in each finite element center.

$$z = a_1 x + a_2 y + a_3 xy + a_4 x^2 + a_5 y^2$$

$$\theta(x,y) = \begin{cases} \tan^{-1}\left(-\dfrac{a_1 + a_3 y + 2a_4 x}{a_2 + a_3 x + 2a_4 y}\right), & a_2 + a_3 x + 2a_4 y \neq 0 \\ \dfrac{\pi}{2}, & a_2 + a_3 x + 2a_4 y = 0 \end{cases} \qquad (4.7)$$

In this method, the fiber angle is supposed to be constant in a finite element so the reference curve can then be defined. Having a_1, a_2, and a_3 equal to zero, a constant curvature path can be defined as in Figure 13.

$$z = x^2 + y^2$$
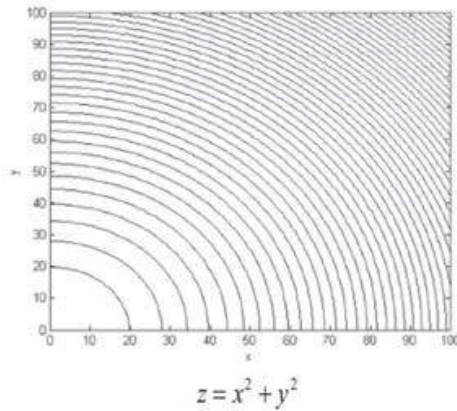
Figure 13: Constant curvature reference curve using polynomial equation [35].

Another strategy which implies a reference curve with a constant curvature on a flat panel is given in [25]. This strategy lies in the variation of the fiber angle between two points, each one having a different fiber angle T_0 and T_1 separated by a distance d. T_0 defines the starting point of this path. Between T_0 and T_1, a constant curvature arc with radius R* is defined (Figure 14).
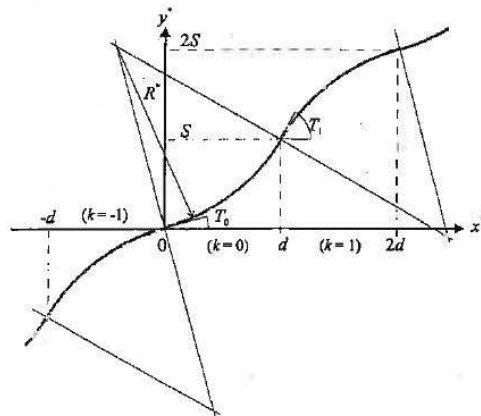
Figure 14: Reference curve based on circular arcs [25].

For a cone, the constant curvature can be computed by keeping κ constant in equation (4.3). A representation of this reference curve is given in Figure 11. The case of a beam and a cylinder is studied respectively in [78] and [8] using the same method. The case of a planar surface is developed in [6] and [53] where the fiber angles follows a constant curvature path from a boundary to the center of the surface.

4.3.2 Linear Variation

Another variable fiber angle layup strategy is based on the linear variation of the fiber directions in the path. This method has been used by [1][1], [4], [5], [9], [24], [25], [26], [35], [38], [51], [52], [61], [62], [63], [72], [73], [74], [78]. This strategy lies in the linear variation of the fiber angle between two points, each one having a different fiber angle T_0 and T_1 separated by a distance d. T_0 defines the starting point of this path. The axis system of fiber orientation is defined by rotating the rosette by an angle φ. This new axis defines a new fiber orientation called r. The fiber path is then defined by φ<T_0|T_1> and varies linearly along r from T_0 to T_1.
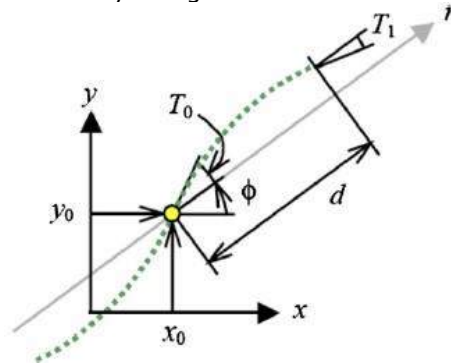
Figure 15: Reference curve with a linear variation [24],[51].

According to Figure 15, one can deduce θ(r) the fiber angle as a function of r in the polar coordinate:

$$\theta(r) = \begin{cases} \phi + (T_0 - T_1) . \dfrac{r}{d} + T_0, & -d \leq r \leq 0 \\ \phi + (T_1 - T_0) . \dfrac{r}{d} + T_0, & 0 \leq r \leq d \end{cases} \qquad (4.8)$$

The reference curve repeats indefinitely with a 2d period until it reaches a boundary.

4.3.3 Nonlinear Variation

Non-linear angle variations have been employed to obtain higher structural performance [5]. Different methods have been used to define the layup trajectories with this non-linear variation and are explained in this section.

4.3.3.1 Free form

First, B-spline curves have been used to define a parametrical equation for reference curves. However, this method has its limits as larger amounts of control points reduce its effectiveness. This results in low-resolution path with bad connectivity between the control points [34].
A Bezier curve, frequently used in computer graphics to model a smooth curve, is another way to define the reference curve with a parametrical equation of the path on the surface using a set of control points [19]. In [43], the Bezier curve is represented with a vector equation including the control points and the junction angles between each point. An example of this equation for a Bezier curve between two control points is given bellow:

$$\vec{B}(t) = (1-t)^2 \, \vec{P_0} + 2(1-t)t\vec{Q_1} + t^2\vec{P_2}, \qquad t \in [0,1] \quad \text{with,} \qquad (4.9)$$

$$\vec{P_0} = (0,0), \qquad (4.10)$$

$$\vec{Q_1} = (\beta_1 a, \beta_1 a \, tan\alpha_0), \qquad (4.11)$$

$$\vec{P_1} = (a, \beta_1 a \, tan\alpha_0 + (1 - \beta_1)a \, tan\alpha_1, \qquad (4.12)$$

Where P_0 is the starting point, P1 is the end point and Q1 is the junction between the two of them; The angles α_0 and α_1 are defined as in Figure 16 and β_1 is the angle variation coefficient which defines the location of the junction point Q_1.
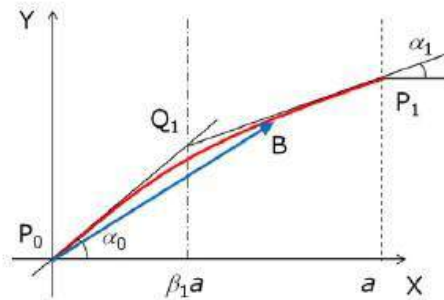
Figure 16: Tow path represented by piecewise quadratic Bezier curves with two control points [43].

One can then deduce the coordinates of any point on the curve:

$$x = (1 - 2\beta_1)t^2 + 2\beta_1 t, \quad 0 \le x, t \le 1 \tag{4.13}$$

$$y = \big((1 - \beta_1)\tan\alpha_1 - \beta_1 \tan\alpha_0\big)t^2 + 2\beta_1 \tan\alpha_0\, t \tag{4.14}$$

It is also possible to add other segments to increase the freedom of the tow path. To do so, a new parameter needs to be introduced which makes the link between the different junction points:
$\gamma = (i - 1 + \beta_i)/N$,
Where i and N are respectively the current segment number and the total number of segments. An example of a tow path between two segments is given Figure 17.
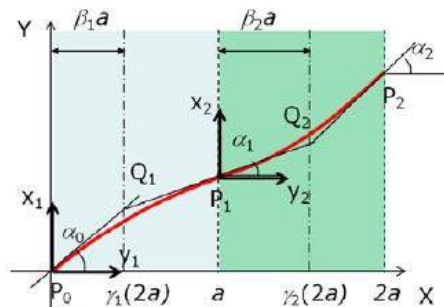
Figure 17: Tow path represented by piecewise quadratic Bezier curves with two segments [43].

In [54], the surface is considered as a bicubic Bezier surface with 16 control points as design perimeters. The control points are forming a mesh and the fiber angle can be written in a cubic polynomial form:

$$s(r) = ar^3 + br^2 + cr + d, \quad and\ r = x\cos(\alpha) + y\sin(\alpha) \tag{4.15}$$

As the fiber angle is constant in a finite element and considering the point $M(x_m, y_m)$ the center of the finite element, the fiber angle within a finite element is:

$$\theta = \tan^{-1}[3a(x_m \cos\alpha + y_m \sin\alpha)^2 + 2b(x_m \cos\alpha + y_m \sin\alpha) + c] + \alpha \tag{4.16}$$

In [47], the reference curve trajectory is optimized following different control points. Indeed, control points are defined on the surface and the fiber angle varies until the compliance is the lowest as possible (*Figure 18*). The optimization problems are resolved thanks to finite difference sensitivities. The curvature of the surface can also be considered in the optimization to decrease the compliance.
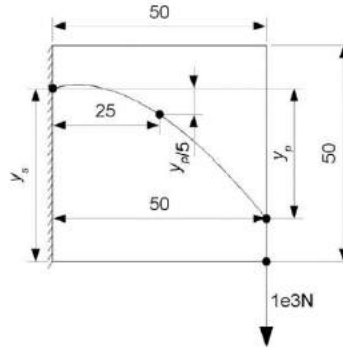
Figure 18: Reference curve optimizing the compliance constraints [47].

4.3.3.2 Polynomial

Multiple research, such as [1],[5],[32],[33], use a mesh and a cubic polynomial function to determine the fiber angle along the surface:

$$f(x,y) = c_{00} + c_{10}x + c_{01}y + c_{20}x^2 + c_{11}xy + c_{02}y^2 + c_{30}x^3 + c_{21}x^2y + c_{12}xy^2 + c_{03}y^3 \qquad (4.17)$$

The different coefficient of the polynomial function can vary with the surface as they determine the surface shape. The fiber angle θ is also considered as constant in a finite element (but can vary from one finite element to another) so it is calculated in the center of the finite element (x_C,y_C):

$$\theta(x_C, y_C) = \tan^{-1}\left(-\frac{\partial f/\partial x}{\partial f/\partial y}\right), \text{ when } \partial f/\partial y = 0, \ \theta = 90° \qquad (4.18)$$

The method used is more efficient than the ones using spline functions [34]. Indeed, the fiber shape is defined in the polynomial functions while, using spline functions, simultaneous equations need to be solved for the same task. The path is then optimized by the genetic algorithm defined in the following section.

In [75], Lagrangian polynomial functions are used to determine the reference curve. The following equation gives the expression of the fiber angle on the surface:

$$\theta(x,y) = \sum_{m=0}^{M-1} \sum_{n=0}^{N-1} T_{mn} \cdot \prod_{m \neq 1}\left(\frac{x - x_i}{x_m x_i}\right) \cdot \prod_{n \neq j}\left(\frac{y - y_j}{y_n - y_j}\right) \qquad (4.19)$$

Where (x_i ,y_j),(x_m,y_n) are the x-y coordinates of reference points. The reference curve is then obtained by resolving the equation at different reference point (Figure 19).

5 COVERAGE STRATEGIES

In this section, the different coverage strategies are detailed. Indeed, three strategies can be used to cover the entire surface. The first one is to compute the different curves independently and the two others are to compute all the other courses path from a reference curve.
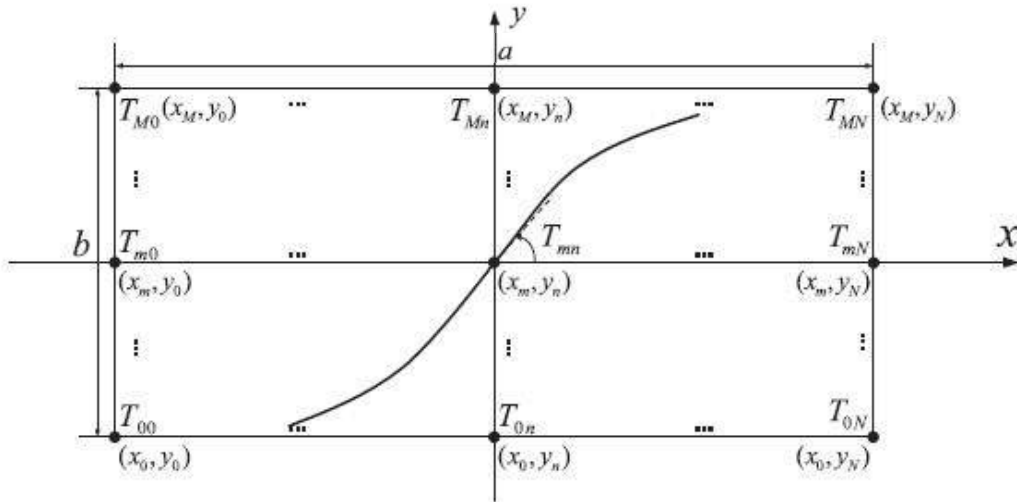
Figure 19: Non-linear path using Lagrangian polynomial function [75].

5.1 Offset curves

The offset curves, or also called parallel curves strategy is the most common one for path planning. Adjacent curves on the surface are computed from the reference curve to achieve total coverage. Tow-paths within a course have to be determined using this method due to the roller mechanism that ensures all tows within a course to be parallel. To explain this coverage strategy, the distinction between the parametrical approach and the usage of a mesh will be investigated.

5.1.1 Using a parametrical approach

To compute the parallel curves parametrically, a closed form solution for continuous planar curves exists by taking equidistant points following the normal vector along the curve. This can be expressed as [70],[71]:

$$\boldsymbol{C}(t): \begin{cases} x(t) = u_c(t) \\ y(t) = v_c(t) \\ z(t) = 0 \end{cases}, \quad \boldsymbol{C_p}(t): \begin{cases} x_p(t) = u_c(t) - d\,\dfrac{v_c'(t)}{\left(u_c'^2(t) + v_c'^2(t)\right)^{1/2}} \\ y_p(t) = v_c(t) + d\,\dfrac{u_c'(t)}{\left(u_c'^2(t) + v_c'^2(t)\right)^{1/2}} \\ z_p(t) = 0 \end{cases} \tag{5.1}$$

where $\boldsymbol{C}(t)$ is the reference curve and $\boldsymbol{C_p}(t)$ is a parallel curve at a distance d from the original, and d can be either a positive or a negative number.

For the case of a general surface, a closed form solution for the parallel curves does not exist in most cases. Hence several algorithms [58],[60],[77] have been developed to compute offset/parallel curves numerically.

For instance, a similar approach for the planar case is used in [58] to find parallel curves by following the vector normal to the reference curve. This vector named **O** (Figure 20) can be found by taking the cross product between the tangent vector to the curve and the normal vector to the surface. Then at a distance d along the vector **O**, a point $\boldsymbol{P'}$ is projected to the surface following the normal vector using a Global Closest Technique. This process is repeated at every point-step along the curve to obtain the new parallel curve. The resulting error from using this technique (Figure 21) is reported to be [58]:

$$Error = d \left(1 - \frac{\psi}{\tan \psi}\right) \tag{5.2}$$

Therefore, the error increases by taking a further offset curve (in the case of wider roller), and in the case of highly curved surface.
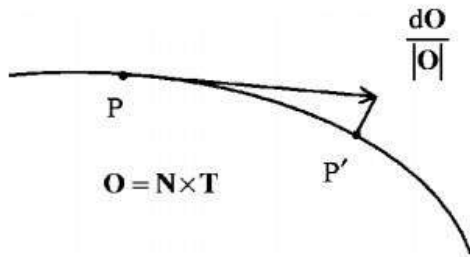
Figure 20: Cross Section of placement surface showing calculation of offset point [58].
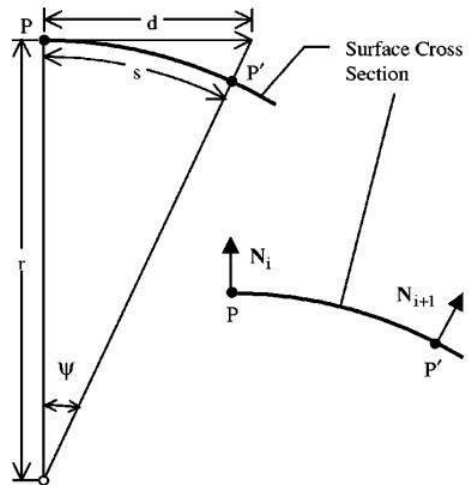
Figure 21: Error associated with placing a point on a surface with circular arc cross section [58].

A more accurate method is presented in [58],[60],[69],[77], by taking the intersection between the plane perpendicular to the curve and the mold surface. To do so, a numerical approach presented in [49] is used to determine the resulting curve. Then, the offset point can be found by taking the required distance along the perpendicular arc. A last step is needed to obtain a complete offset path in the case where the reference path is shorter than the offset one that does not reach a boundary. In this case, the offset curve is completed by interpolating the last point from the calculated ones until it reaches the boundary.
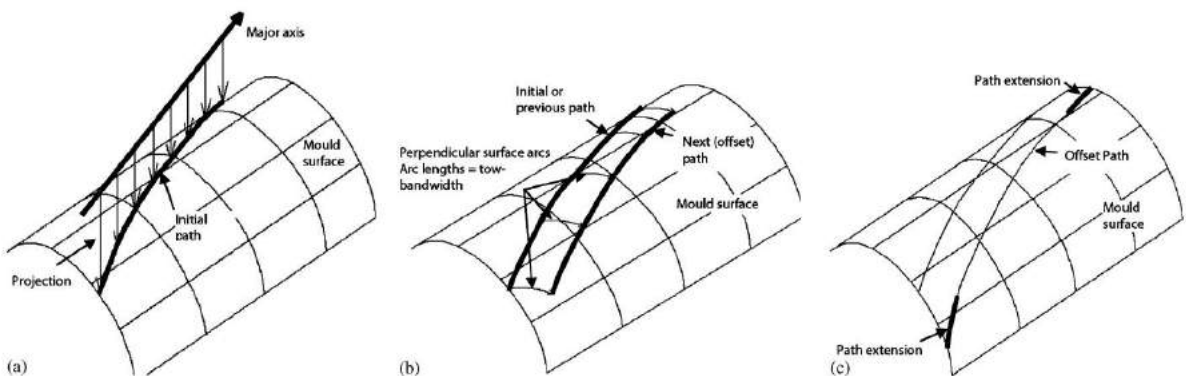
Figure 22: (a) Initial path generation, (b) Curve Offset, (c) Path extension [60].

Three other methods are presented in [23] to compute parallel curves on a NURBS surface. The first method named section curves is similar to the ones presented in [58],[60],[69],[77]. The other two consist of generating orthogonal curves to the reference by either taking vector-field curves or geodesic curves. Once the orthogonal curve is defined in either of these methods, the offset points

can be calculated at the required distance from the reference curve, and finally the new parallel curve is obtained by interpolating these points.

The advantage of computing parallel curves is that the offset curves are equidistant so there are no gaps or overlaps between the paths or the courses during the layup process.
On another hand, considering a complex surface, the fibers directions in the offset curve can change. To optimize the fiber direction and to avoid a too important deviation of these angles, [16] considers an interval of direction and tests the deviation of the offset fibers while the fiber direction in the reference path varies. The reference curve which conserves the most the fiber directions in the offset path constant is then selected.

5.1.2   Using a mesh: Fast Marching Method

This method has been introduced by [11],[47] and is based on the Eikonal equation (Figure *23*). This equation is mostly used in optic and is used to calculate the propagation of a wave with a particular speed. Hence, from a wave, one can calculate the different position of this wave at every time once it starts propagating.

This method starts from a random reference curve on the surface. First, the reference curve needs to be discretized. The intersection points between the mesh and the reference curve form the discretized reference path. For initialization, all these points have a time value of 0. Then, the reference curve is propagated at a defined speed so every node of the mesh will hit the propagated curve at a certain time. Moreover, knowing the time value of two nodes of one mesh triangle, we can calculate the time value of the last node. Indeed, on an accurate triangular mesh *Figure 24*, knowing the time values of the points A and B respectively T_A and T_B, one can find the time value of C T_C.

a) Define the mesh of the structure   b) Trace the reference curve

c) Solve the Eikonal Equation
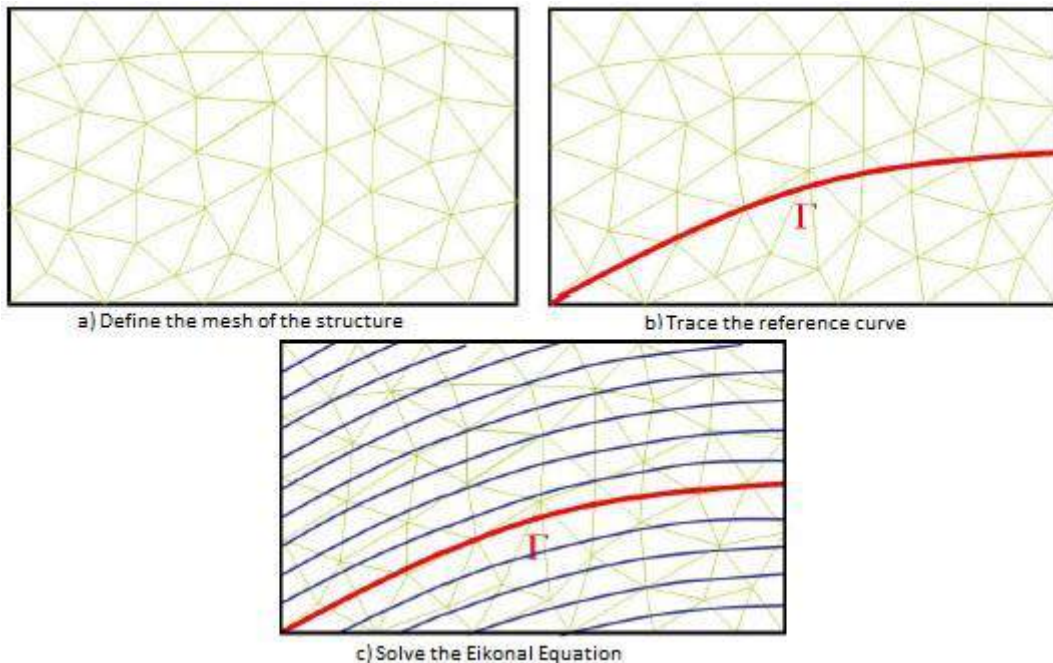
Figure 23: The different step of the Fast Marching Method to offset a reference curve [11].
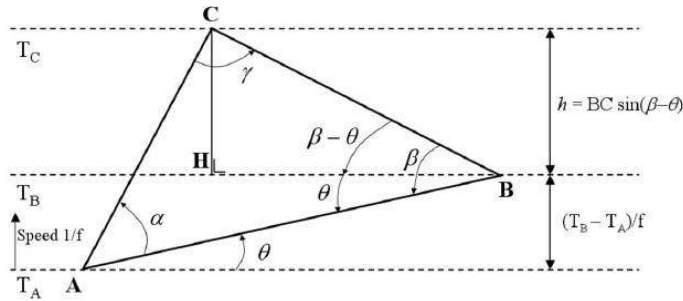
Figure 24: Finding TC knowing TA and TB [11].

Using the following equations and with 1/f the propagation speed of the reference curve:

$$\theta = \arcsin\left(\frac{T_B - T_A}{f.AB}\right) \tag{5.3}$$

$$h = BC \sin(\beta - \theta) \tag{5.4}$$

One can deduce T$_C$:

$$T_C = h.f + T_B \tag{5.5}$$

To propagate this calculation, the Fast Marching Method explained in [10] is used. The principle of this method is to look for the neighbor nodes of the one with the lowest time value. Then, all the nodes around this one are updated. The initial node won't be considered anymore and the update is done from the next node with the lowest value. It is important to notice that the time value of each node is updated only if the calculated value is smaller than the previous one.

Once all the nodes time values are known, for each time value an offset curve of the reference curve can be drawn. Indeed, knowing the speed and the time, an offset curve with the proper distance from the reference curve can be found. Indeed, the offset curve joins the different iso-value points. However, to obtain a real parallel curve, the reference curve must be considered as infinite (it means that it goes through the boundaries) when propagated with the fast marching method. Indeed, if the reference path is not extended, the offset curves won't necessarily be parallel to it in every points (Figure 25).
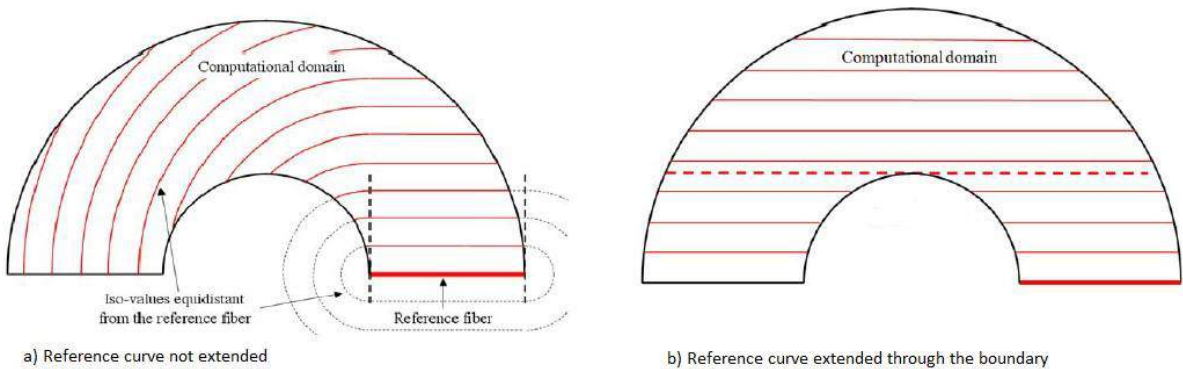
Figure 25: Difference between a non-extended and an extended reference curve [11].

Thanks to this method, equidistant curves are obtained. This avoids gap and overlaps but other default linked to the steering can be observed. The direction of the fiber will be well respected if the reference curve follows the right direction.

5.2 Shifted Curves

In [6],[7],[8],[25],[38],[42],[50],[51],[63],[68],[72],[73], the reference curve is simply shifted in along its perpendicular direction on the surface by applying a translation. The advantage of this method is its simplicity but the inconvenient is that, on a complex surface, the fiber directions of the offset path are not guaranteed and the presence of gaps and overlaps is possible.
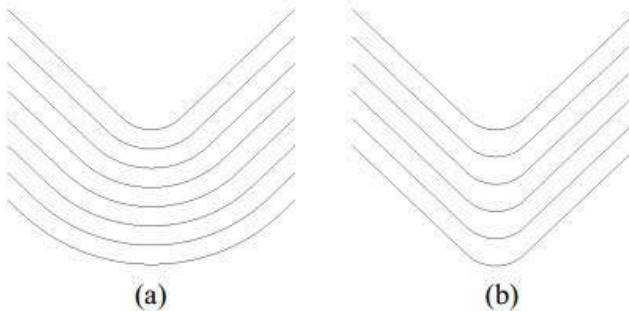
Figure 26: Tow path definition: (a) Parallel method, (b) Shifting method [42].
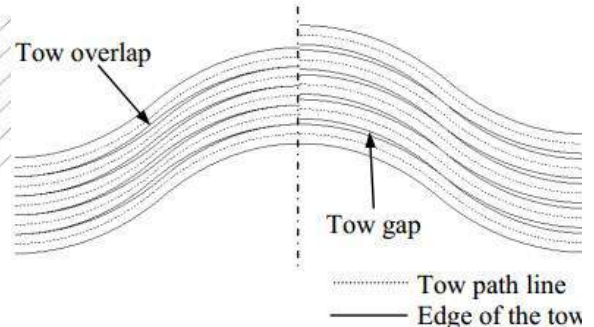
Figure 27: Gap and Overlap resulted in the shifting method [42].

a. Independent curves

Another possibility to cover the entire surface is to draw the different curves independently. Regarding complex surfaces, independent curves can be a solution to limit extreme steering. To cover the surface, it is possible to draw the courses staggered one to another with a constant length and with a different direction [58]. Indeed, if the surface is a complex one, the different courses are not necessarily parallel to each other if they all respect the required direction. This will induce gaps and overlaps
Figure 28.
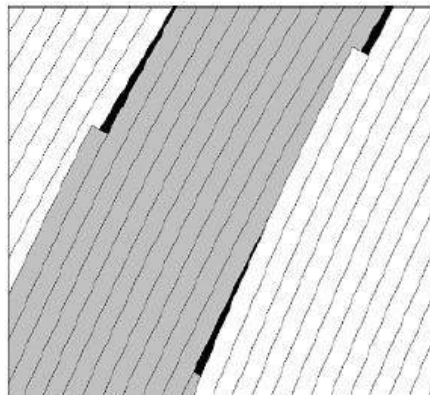
Figure 28: Gaps and overlaps induced by independent direction curves [58].

Another strategy based on the same principle, which is independent fibers following the right direction, but which also controls the presence of gaps and overlaps which requires many short courses. This strategy has been studied by [20] for a conical surface Figure 29. The drawback of this method is that it needs a lot of short independent courses so the structure is less resistant to constraints because of the important number of cuts.
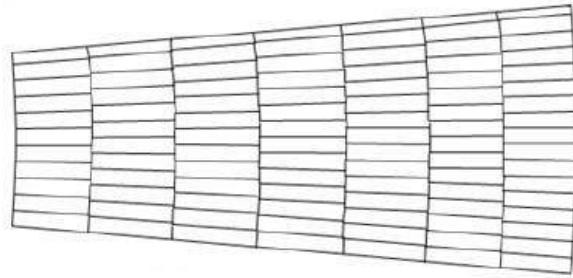
Figure 29: Succession of short independent courses to cover a conical surface [20].

6   DISCUSSION AND SUMMARY

This review gave the different layup strategies present in the literature to compute a reference path and to cover the surface. This section is a summary of this review. A geometry benchmark as a Timeline of the different publication are presented in this section as well as a discussion for further work.

6.1   Geometry Benchmark and Timeline

In this section, a geometry benchmark is drawn (
Figure 30). This benchmark allows the reader to find which AFP layup strategy corresponding to each geometry have been found in the literature. The references corresponding to each type of strategies are also summarized in this benchmark. Then the different dimensions of the surfaces encountered in the literature are summarized. Finally, a timeline of the different publications ranged by their geometry is presented.
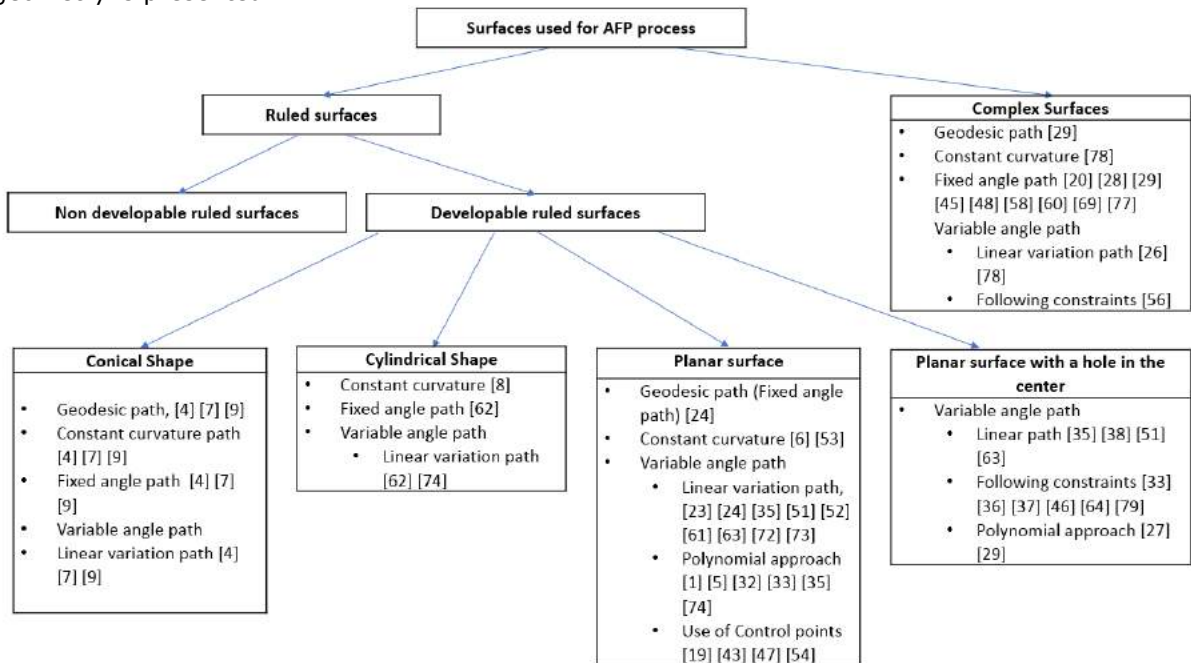
Figure 30: Geometry Benchmark.

In the
Table *2*-
Table *6*, the different test surfaces are summarized. Future studies on layup strategies for the AFP process should be compared to the results obtained on the surfaces below.

Dimensions (mm)	References (Dates)
300x300	[6] (2009)
254x406	[53] (2014)
508x381	[63] (2002) [51] (2008)
660,4x622,3	[73] (2002) [72] (2001)
50x50	[47] (2015)
305x76,2	[61] (2014)
254x254	[52] (2012) [75] (2012)
1000x500	[54] (2016)
200x80	[35] (2016)
Length/Width	References
1	[1](2008) [34] (2011) [33] (2013)

Table 2: Planar surfaces.

Dimensions (mm)	Diameter (mm)	Hole position	Reference
508x381	38,1	Center	[38] (2003) [63] (2002)
	76,2	Center	[38] (2003) [63] (2002) [50] (2007)
140x70	12,7	Center	[64] (2000)
300x90	40	x = 250, y = 45	[46] (2006)
200x200	50	Center	[36] (2005)
300x60	10	Center	[79] (2017)
200x200	80	Center	[35] (2016)
700x100	50	x = y = 0	[33] (2013)
Length/Width	Width/Diameter	Hole position	Reference
1	3,33	Center	[37] (1991)
2	1,67		

Table 3: Planar surfaces with a hole.

Small radius (cm)	Large radius (cm)	Axial length (cm)	Cone angle (°)	References
6	10	10	21,8	[7] (2007) [4] (2010)
6	10	25	9,09	
6	10	40	5,71	
8	10	10	11,31	
8	10	25	4,57	
8	10	40	2,86	
10	10	10	0	

10	10	25	0	
10	10	40	0	
30	30	72,5	0	
30	35	100	2,86	
12,5	80	80,4	40	[7] (2007) [4] (2010) [9] (2009)
30	60	200		[47] (2015)

Table 4: Conical Surfaces.

Diameter (in)	Length (in)	Reference
17	34	[74] (2009)
148	20	[62] (1998)
24	32	[8] (2010)

Table 5: Cylindrical Surfaces.

Beam		References
Length	2,032 m	[78] (2011) [26] (2012)
Width	0,254 m	
Depth	0,068 m	
Wall Thickness	0,01 m	
Y shape		
Diameter	45 mm	[29] (2017)
Length lower branch	200 mm	
Length of upper branches	120 mm	
Angle between the branches	80° to 150°	

Table 6: Complex surfaces.

A timeline of all the publications found in the Geometry Benchmark is presented in Tab.7. In the top hand-left corner, the different geometry and their colors in the Timeline are registered. One can notice that some strategies used for the complex surfaces can also be used for any type of surfaces as their method to compute a reference path is general enough.

6.2   Discussion and future work

In this section, future works and discussions around the work done in this review will be provided.

a) In this review, layup strategies exclusively based on the mechanical properties and their optimization are not explained. These strategies could be incorporated in the section 5 (coverage strategies). In some cases, the paths follow the principal stress ([73],[74])or the principal load ([68], [75]) constraint on the surface. Other strategies use a mesh description of the surface and use an optimizer algorithm to determine the optimal angle orientation in each finite element of the mesh. One of this algorithm is used in [35], [56], [58], [69] and [72]. Then methods such in [77] or the use of streamlines in [49] can be used to compute a path based on the angle found previously.

b) CAD software such as Vericut [14] from CG Tech, ICPS [12] from Ingersoll Machine Tools, Truplan [3] from Autodesk, CATFiber [15] from Coriolis, and MAG by ACES [22] can compute some of the strategies exposed in this review.

For the reference curve, all these software are able to compute a fix angle reference curve on the surface. They also allow the user to define a seed curve which will be projected on the surface such as it has been explained in section 4.1.2. Doing so, one can compute any path on the tool surface. Vericut [14] and CATFiber [15] software can also compute a geodesic path on the surface. Finally, in ICPS [12], Vericut [14], and MAG [22], a steering path can be computed. This path is a fixed angle path but the different software makes sure that the steering is valid at any point of the course.

Concerning the coverage strategies, each software is able to compute independent and parallel curves.

Table 7 below summarizes which layup strategies are computed by each software.

Layup Strategies	Geodesic path	Fix angle path	Steering path	Seed curve projection	Independent curves	Parallel curves
ICPS		X	X	X	X	X
Vericut	X	X	X	X	X	X
CATFiber	X	X		X	X	X
MAG		X	X	X	X	X
Truplan		X		X	X	X

Table 7: Layup Strategies associated to their software.

a) Knowing all the different layup strategies for computing the reference curve and to cover the surface, future works will be able to determine which strategy is the most optimal. But before that, the question of why a layup strategy is better than another needs to be answer. The authors provide in

b) Table 9 a possible way of comparing the different strategies. First the percentages of gaps and overlaps on the surface which are linked to the right coverage of the latter can be compared. Then the different notable defects induced by each strategy are given. Finally, regarding to the requirement specification of the structure and the results, the different layup strategies can be ranked. The algorithm, once applied, will compute the overall % of gaps to be found in the layup, if the corresponding reference/coverage is applied. Similarly, we compute the % of overlaps. Subsequently, physic based and other models can be implemented to anticipate the presence of notable defect. One might integrate the concepts presented in [70] and [71] to predict wrinkles. Finally, weighting algorithms can be used to determine the overall rank of the selected combination.

7   AKNOWLEDGEMENTS

Guillaume Rousseau, http://orcid.org/0000-0003-3751-4366
Roudy Wehbe, http://orcid.org/0000-0003-0615-7634
Joshua Halbritter, http://orcid.org/0000-0001-5747-2875
Ramy Harik, http://orcid.org/0000-0003-1452-9653

Year	Geometry	Title	Author	References
1991	FLAT PANEL WITH HOLE	*Use of Curvilinear fiber format in composite structure design*	Hyer et al	[37]
1996	COMPLEX SURFACE BUT CAN BE USED FOR ANY TYPE OF SURFACE	*Design and manufacture of advanced composite aircraft structures using automated tow placement*	Land	[45]
1998	CYLINDER	*Analysis and design of variable stiffness composite cylinders*	Tatting	[62]
2000	FLAT PANEL WITH HOLE	*On the design, manufacturing and testing of trajectorial fiber steering for carbon fibre composite laminates*	Tosh et al	[64]
2001	FLAT PANEL	*Thermal Testing of Tow-Placed, Variable Stiffness Panels*	Wu et al	[72]
2002	FLAT PANEL WITH AND WITHOUT HOLE	*Design and manufacture of elastically tailored tow placed plates*	Tatting et al	[63]
2002	FLAT PANEL	*Structural Response of Compression-Loaded Tow-Placed, Variable Stiffness Panels*	Wu et al	[73]
2003	FLAT PANEL WITH HOLE	*Optimization of elastically tailored tow-placed plates with holes*	Jegley et al	[38]
2003	FLAT PANEL	*Optimum design of composite structures with curved fiber courses*	L. Parnas et al	[54]
2004	COMPLEX SURFACE BUT CAN BE USED FOR ANY TYPE OF SURFACE	*Approximate Geometric Methods in Application to the Modeling of Fiber Placed Composite Structures*	Schueler et al	[58]
2005	FLAT PANEL WITH HOLE	*Optimization of fiber orientations near a hole for increased load-carrying capacity of composite laminates*	Huang et al	[36]
2005	FLAT PANEL	*Tow-placement technology and fabrication issues for laminated composite structures*	Gürdal et al	[25]
2006	FLAT PANEL WITH HOLE	*Optimisation of fiber steering in composite laminates using a genetic algorithm*	Legrand et al	[46]
2007	FLAT PANEL WITH HOLE	*Progressive Failure Analysis of Tow-Placed, Variable Stiffness Composite Panels*	Lopes et al	[50]
2007	COMPLEX SURFACE BUT CAN BE USED FOR ANY TYPE OF SURFACE	*Process and design considerations for the automated fiber placement process*	Favaloro et al	[20]
2007	COMPLEX SURFACE BUT CAN BE USED FOR ANY TYPE OF SURFACE	*Trajectory generation for open-contoured structures in robotic fibre placement*	Shirinzadeh et al	[60]
2007	COMPLEX SURFACE BUT CAN BE USED FOR ANY TYPE OF SURFACE	*Intersection of a ruled surface with a free-form surface*	X. Wang et al	[69]
2007	CONE	*Design of Variable-Stiffness Conical Shells for Maximum Fundamental Eigenfrequency*	Blom et al	[7]
2008	FLAT PANEL	*Variable-stiffness composite panels: Buckling and first-ply failure improvements over straight-fibre laminates*	Lopes et al	[51]
2008	FLAT PANEL	*Design tailoring for pressure pillowing using tow-placed steered fibers*	Alhajahmad et al	[1]
2008	FLAT PANEL	*Variable-stiffness composite panels: effects of stiffness variation on the in-plane and buckling response*	Gürdal et al	[24]
2009	FLAT PANEL	*A Theoretical Model to Study the Influence of Tow-drop Areas on the Stiffness and Strength of Variable-stiffness Laminates*	Blom et al	[6]

2009	CONE	*Fiber path definitions for elastically tailored conical shells*	Blom et al	[9]
2009	CYLINDER	*Design and manufacturing of tow-steered composite shells using fiber placement*	Wu et al	[74]
2010	FLAT PANEL	*Optimization of course locations in fiber-placed Panels for general fiber angle distributions*	Blom et al	[5]
2010	CONE AND CYLINDER	*Structural performance of fiber-placed, variable-stiffness composites and cylindrical shells*	Blom et al	[4]
2010	CYLINDER	*Optimization of a composite cylinder under bending by tailoring stiffness properties in circumferential direction*	Blom et al	[8]
2011	FLAT PANEL	*Vibration design of laminated fibrous composite plates with local anisotropy induced by short fibers and curvilinear fibers*	Honda et al	[32]
2011	COMPLEX SURFACE	*Research on Fiber Placement Trajectory Design Algorithm for the Free-Form Surface With Given Ply Orientation Information*	Peiyuan et al	[56]
2011	COMPLEX SURFACE	Curvilinear fiber optimization tools for design of thin walled beams	Zamani et al	[78]
2012	COMPLEX SURFACE BUT CAN BE USED FOR ANY TYPE OF SURFACE	*A path planning algorithm of closed surface for fiber placement*	Han et al	[28]
2012	FLAT PANEL	*Surrogate-based multi-objective optimization of a composite laminate with curvilinear fibers*	Nik et al	[52]
2012	FLAT PANEL	*Continuous tow shearing for manufacturing variable angle tow composites*	Kim et al	[43]
2012	FLAT PANEL	*Buckling analysis and optimisation of variable angle tow composite Plates*	Wu et al	[75]
2012	COMPLEX SURFACE	*Curvilinear fiber optimization tools for aeroelastic design of composite wings*	Haddadpour et al	[26]
2013	FLAT PANEL WITH AND WITHOUT HOLE	*Multi-objective optimization of curvilinear fiber shapes for laminated composite plates using NSGA-II*	Honda et al	[33]
2014	FLAT PANEL	*Optimization of variable stiffness composites with embedded defects induced by Automated Fiber Placement*	Nik et al	[53]
2014	COMPLEX SURFACE BUT CAN BE USED FOR ANY TYPE OF SURFACE	*A Placement Path Planning Algorithm Based on Meshed Triangle for Carbon Fiber Reinforced Composite Components with Revolved Shapes*	Li et al	[48]
2014	COMPLEX SURFACE BUT CAN BE USED FOR ANY TYPE OF SURFACE	*An accurate approach to roller path generation for robotic fibre placement of freeform surface composites*	Yan et al	[77]
2014	FLAT PANEL	*Aeroelastic benefits of tow steering for composite plates*	Stanford et al	[61]
2014	FLAT PANEL	*Curves and surfaces for computer-aided geometric design*	Farin	[19]
2015	FLAT PANEL	*Optimization of composite structures with curved fiber trajectories*	Lemaire et al	[47]
2016	FLAT PANEL WITH AND WITHOUT HOLE	*An efficient reanalysis assisted optimization for variable-stiffness composite design by using path functions*	Huang et al	[35]
2017	FLAT PANEL WITH HOLE	*Fiber path optimization based on a family of curves in composite laminate with a center hole*	Zhu et al	[79]
2017	COMPLEX SURFACE	*Feasibility study of robotic fibre placement on intersecting multi-axial revolution surfaces*	Hély et al	[29]

Table 8: Publication Timeline concerning layup strategies for the AFP process.

Geometry of the surface:					
Strategy for the reference curve	Coverage Strategy	Coverage percentage		Notable Defects	Ranking
		% of Gaps	% of Overlaps		
Geodesic path	Fast Marching Method				
	Parametrical Parallel curves				
	Shifted curves				
	Independent curves				
Constant Curvature	Fast Marching Method				
	Parametrical Parallel curves				
	Shifted curves				
	Independent curves				
Linear Variation	Fast Marching Method				
	Parametrical Parallel curves				
	Shifted curves				
	Independent curves				
Use of control points	Fast Marching Method				
	Parametrical Parallel curves				
	Shifted curves				
	Independent curves				
Following the constraints	Fast Marching Method				
	Parametrical Parallel curves				
	Shifted curves				

	Independent curves				

Table 9: Table to find the optimal layup strategy.

REFEFERENCES

[1] Alhajahmad, A.; Abdalla, M.; Gürdal, Z.: Design tailoring for pressure pillowing using tow placed steered fibers, Journal of Aircraft, 45(2), 2008, 630-640. https://doi.org/10.2514/1.32676

[2] August, Z.; Ostrander, G.; Michasiow, J.; Hauber, D.: Recent developments in automated fiber placement of thermoplastic composites, SAMPE J, 50(2), 2014, 30-37.

[3] Autodesk, https://www.autodesk.com/products/truplan/overview, Truplan Software.

[4] Blom, A.: Structural performance of fiber-placed, variable-stiffness composite conical and cylindrical shells, Delft University of Technology, 2010.

[5] Blom, A.; Abdalla, M.; Gürdal, Z.: Optimization of course locations in fiber-placed panels for general fiber angle distributions, Composites Science and Technology, 70(4), 2010, 564-570. https://doi.org/10.1016/j.compscitech.2009.12.003

[6] Blom, A.; Lopes, C.; Kromwi, P.; Gürdal, Z.; Camanho, P.: A theoretical model to study the influence of tow-drop areas on the stiffness and strength of variable-stiffness laminates, Journal of Composite Materials, 43(5), 2009, 403-425. https://doi.org/10.1177/0021998308097675

[7] Blom, A.; Setoodeh, S.; Hol, J.; Gürdal, Z.: Design of Variable-Stiffness Conical Shells for Maximum Fundamental Eigenfrequency, Computers and Structures, 86(9), 2007, 870–878. https://doi.org/10.1016/j.compstruc.2007.04.020

[8] Blom, A.; Stickler, P.; Gürdal, Z.: Optimization of a composite cylinder under bending by tailoring stiffness properties in circumferential direction, Composites: Part B, 41(2), 2010, 157–165. https://doi.org/10.1016/j.compositesb.2009.10.004

[9] Blom, A.; Tatting, B.; Hol, J.: Fiber path definitions for elastically tailored conical shells, Composites: Part B, 40(1), 2009, 77–84. https://doi.org/10.1016/j.compositesb.2008.03.011

[10] Brampton, C.; Kim, H.: Optimization of tow steered fibre orientation using the level set method, 10th World Congress on Structural and Multidisciplinary Optimization. Orlando FL, 2013.

[11] Bruyneel, M.; Zein, S.: A modified fast marching method for defining fiber placement trajectories over meshes, Computers & Structures, 125, 2013, 45-52. https://doi.org/10.1016/j.compstruc.2013.04.015

[12] Camozzi Machine Tools, http://www.camozzimachinetools.com/en/camozzigroup/machine-tools/home, iCPs Software.

[13] Chen, H.; Fuhlbrigge, T.; Li, X.: A review of CAD-based robot path planning for spray painting, Industrial Robot, An International Journal, 36(1), 2009, 45-50.

[14] CGTech, https://www.cgtech.com/products/about-vericut, VERICUT Software.

[15] Coriolis, http://www.coriolis-software.com/products-software/catfiber-for-catia.html, CATFiBer Software.

[16] Debout, P.: Calcul de trajets de dépose dans le cadre de la fafrication de pieces aéronautiques, Université Blaise Pascal-Clermont-Ferrand II: Doctoral dissertation, 2010.

[17] DeVlieg, R.; Jeffries, K.; Vogeli, P.: High-speed fiber placement on large complex structures (No. 2007-01-3843), SAE Technical Paper, 2007.

[18] Dirk, H.; Ward, C.; Potter, D.: The engineering aspects of automated prepreg layup: History, present and future, Composites Part B: Engineering, 43(3), 2012, 997-1009. https://doi.org/10.1016/j.compositesb.2011.12.003

[19] Farin, G.: Curves and surfaces for computer-aided geometric design: a practical guide, Elsevier, 2014.

[20] Favaloro, M.; Hauber, D.: Process and design considerations for the automated fiber placement process, ADC Acquisition Company, presented at the SAMPE 2007 fall technical conference. Cincinnati, OH, 2007.

[21] Felderhoff, K.; & Steiner, K.: A new compact robotic head for thermoplastic fiber placement, Advanced Materials: Performance Through Technology Insertion, 38, 1993, 138-149.

[22] Fives, http://metal-cutting-composites.fivesgroup.com/products/composites/composites-systems.html, MAG Software.

[23] Gálvez, A.; Iglesias, A.; & Puig-Pey, J.: Computing parallel curves on parametric surfaces, Applied Mathematical Modelling, 38(9), 2014, 2398-2413. https://doi.org/10.1016/j.apm.2013.10.042

[24] Gürdal, Z.; Tatting, B.; Wu, C.: Variable stiffness composite panels: effects of stiffness variation on the in-plane and buckling response, Composites Part A: Applied Science and Manufacturing, 39(5), 2008, 911-922. https://doi.org/10.1016/j.compositesa.2007.11.015

[25] Gürdal, Z.; Tatting, B.; Wu, K.: Tow-placement technology and fabrication issues for laminated composite structures, Proceedings of the Aiaa/Asme/Asce/Ahs/Asc structures, 46th structural dynamics & materials conference, 2005. https://doi.org/10.2514/6.2005-2017

[26] Haddadpour, H.; Zaman, Z.: Curvilinear fiber optimization tools for aeroelastic design of composite wings, Journal of Fluids and Structures, 33, 2012, 180-190. https://doi.org/10.1016/j.jfluidstructs.2012.05.008

[27] Harik, R.; Saidy, C.; Williams, S.; Gurdal, Z.; Grimsley, B.: Automated fiber placement defect identity cards: cause, anticipation, existence, significance, and progression, Submission to SAMPE 2018 Conference & Exhibition, Long Beach, California, US, 21 – 24 May 2018

[28] Han, Z. Y.; Fu, Q. Q.; Yang, F.; Fu, Y. Z.; Fu, H. Y.: A path planning algorithm of closed surface for fiber placement, Proceedings of the 1st International Conference on Mechanical Engineering and Material Science, Atlantis Press, December 2012. https://doi.org/10.2991/mems.2012.100

[29] Hély, C.; Birglen, L.; Xie, W.-F.: Feasibility study of robotic fibre placement on intersecting multi-axial revolution surfaces, Robotics and Computer–Integrated Manufacturing, 48, 2017, 73–79. https://doi.org/10.1016/j.rcim.2017.02.005

[30] Henne, F.; Ehard, S.; Kollmannsberger, A.; Hoeck, B.; Sause, M.; Obermeier, G.; Drechsler, K.: Thermoplastic in-situ fiber placement for future solid rocket motor casing manufacturing, SAMPE Europe SETEC.

[31] Heraus. (2017, Juillet 12). humm3™ - Intelligent heat for Automated Fibre Placement (AFP). Retrieved 07 12, 2017, from https://www.heraeus.com/en/hng/products_and_solutions/arc_and_flash_lamps/humm_3.aspx

[32] Honda, S.; Narita, Y.: Vibration design of laminated fibrous composite plates with local anisotropy induced by short fibers and curvilinear fibers, Composite Structures, 93(2), 2011, 902-910. https://doi.org/10.1016/j.compstruct.2010.07.003

[33] Honda, S.; Igarashi, T.; Narita, Y.: Multi-objective optimization of curvilinear fiber shapes for laminated composite plates by using NSGA-II., Composites Part B: Engineering, 45(1), 2013, 1071-1078. https://doi.org/10.1016/j.compositesb.2012.07.056

[34] Honda, S.; Narita, Y.; Sasaki, K.: Maximizing the fundamental frequency of laminated composite plates with optimally shaped curvilinear fibers, Journal of System Design and Dynamics, 3(6), 2009, 867-876. https://doi.org/10.1299/jsdd.3.867

[35] Huang, G.; Wang, H.; Li, G.: An efficient reanalysis assisted optimization for variable-stiffness composite design by using path functions, Composite Structures, 153, 2016, 409–420. https://doi.org/10.1016/j.compstruct.2016.06.043

[36] Huang, J.; Haftka, R.: Optimization of fiber orientations near a hole for increased load-carrying capacity of composite laminates, Structural and Multidisciplinary Optimization, 30(5), 2005, 335-341. https://doi.org/10.1007/s00158-005-0519-z

[37] Hyer, M.; Charette, R.: Use of curvilinear fiber format in composite structure design, AIAA journal, 29(6), 1991, 1011-1015. https://doi.org/10.2514/3.10697

[38] Jegley, D. C.; Tatting, B. F.; Gürdal, Z.: Optimization of elastically tailored tow-placed plates with holes, American Institute of Aeronautics and Astronautics, 2003. https://doi.org/10.2514/6.2003-1420

[39] Jirka, T.; Václav, S.: Gradient vector estimation and vertex normal computation, Poland: Szczyrk int.workshop, technical report no. DCSE/TR-2002-08, 2002.

[40] Kelly, D.: Load path calculations and applications using finite element analysis, Proceedings of the First Australasian Congress on Applied Mechanics: ACAM-96. Institution of Engineers. Australia, 1996.

[41] Khan, S.: Thermal control system design for automated fiber placement process, Concordia University: Doctoral dissertation, 2011.

[42] Kim, B.; Hazra, K.; Weaver, P.; Potter, K.: Limitations of fibre placement techniques for variable angle tow composites and their process-induced defects, Proceedings of the 18th international conference on composite materials. Jeju, KR, 2011.

[43] Kim, B.; Potter, K.; Weaver, P.: Continuous tow shearing for manufacturing variable angle tow composites, Composites Part A: Applied Science and Manufacturing, 43(8), 2012, 1347-1356. https://doi.org/10.1016/j.compositesa.2012.02.024

[44] Konrad, K.: Automated fiber placement systems overview, Transactions of the institute of aviation, 245(4), 2016, 52-59.

[45] Land, I.: Design and manufacture of advanced composite aircraft structures using automated tow placement, Massachusetts Institute of Technology: Doctoral dissertation, 1996.

[46] Legrand, X.; Kelly, D.; Crosky, A.; Crépin, D.: Optimisation of fibre steering in composite laminates using a genetic algorithm, Composite structures, 75(1), 2006, 524-531. https://doi.org/10.1016/j.compstruct.2006.04.067

[47] Lemaire, E.; Samih, Z.; Bruyneel, M.: Optimization of composite structures with curved fiber trajectories, Composite Structures, 131, 2015, 895-904. https://doi.org/10.1016/j.compstruct.2015.06.040

[48] Li, L.; Wang, X.; Xu, D.; Tan, M.: A placement path planning algorithm based on meshed triangles for carbon fiber reinforce composite component with revolved shape, International Journal on Control Systems and Applications (IJCS), 1(1), 2014, 23-32.

[49] Limaiem, A.; Trochu, F.: Geometric algorithms for the intersection of curves and surfaces, Computers & graphics, 19(3), 1995, 291-403. https://doi.org/10.1016/0097-8493(95)00009-2

[50] Lopes, C.; Camanho, P. P.; Gürdal, Z.; Tatting, B. F.: Progressive failure analysis of tow-placed, variable-stiffness composite panels, International Journal of Solids and Structures, 44(25), 2007 8493-8516. https://doi.org/10.1016/j.ijsolstr.2007.06.029

[51] Lopes, C.; Gürdal, Z.; Camanho, P.: Variable-stiffness composite panels: Buckling and first-ply failure improvements over straight-fibre laminates, Computers and Structures, 86(9), 2008, 897–907. https://doi.org/10.1016/j.compstruc.2007.04.016

[52] Nik, M.; Fayazbakhsh, K.; Pasini, D.; Lessard, L.: Surrogate-based multi-objective optimization of a composite laminate with curvilinear fibers, Composite Structures, 94(8), 2012, 2306–2313. https://doi.org/10.1016/j.compstruct.2012.03.021

[53] Nik, M.; Fayazbakhsh, K.; Pasini, D.; Lessard, L.: Optimization of variable stiffness composites with embedded defects induced by automated fiber placement, Composite Structures, 107, 2014, 160–166. https://doi.org/10.1016/j.compstruct.2013.07.059

[54] Parnas, L.; Oral, S.; Ceyhan, Ü.: Optimum design of composite structures with curved fiber courses, Composites Science and Technology, 63, 2003, 1071–1082. https://doi.org/10.1016/S0266-3538(02)00312-3

[55] Patrikalakis, N.; Maekawa, T.: Shape interrogation for computer aided design and manufacturing, Springer Science & Business Media, 2001.

[56] Peiyuan, W.; Yong, L.; Xianfeng, W.; Jun, X.: Research on fiber placement trajectory design algorithm for the free-form surface with given ply orientation information, Polymers & Polymer Composites, 19(2/3), 2011, 203.

[57] Sabido, A.; Bahamonde, L.; Harik, R.; van Tooren, MJL.: Maturity assessment of the laminate variable stiffness design process, Composite Structures 160, 2017, 804-812. https://doi.org/10.1016/j.compstruct.2016.10.081

[58] Schueler, K.; Miller, J.; Hale, R.: Approximate geometric methods in application to the modeling of fiber placed composite structures, Journal of Computing and Information Science in Engineering, 4, 2004, 251-256. https://doi.org/10.1115/1.1736685

[59] Shirinzadeh, B.; Alici, G.; Foong, C.; Cassidy, G.: Fabrication process of open surfaces by robotic fibre placement, Robotics and Computer-Integrated Manufacturing, 20(1), 2004, 17-28. https://doi.org/10.1016/S0736-5845(03)00050-4

[60] Shirinzadeh, B.; Cassidy, G.; Oetomo, D.; Alici, G.; Ang Jr, M.: Trajectory generation for open-contoured structures in robotic fibre placement, Robotics and Computer-Integrated Manufacturing, 23(4), 2007, 380-394. https://doi.org/10.1016/j.rcim.2006.04.006

[61] Stanford, B.; Jutte, C.; Wu, K.: Aeroelastic benefits of tow steering for composite plates, Composite Structures, 118, 2014, 416–422. https://doi.org/10.1016/j.compstruct.2014.08.007

[62] Tatting, B.: Analysis and design of variable stiffness composite cylinders, Blacksburg, Virginia, USA: Ph. D. Thesis, Virginia Polytechnic Institute and State University, 1998.

[63] Tatting, B. F.; Gürdal, Z.; Jegley, D. C.: Design and manufacture of elastically tailored tow placed plates, Virginia: Langley Research Center, 2002.

[64] Tosh, M. W.; Kelly, D. W.: On the design, manufacture and testing of trajectorial fibre steering for carbon fibre composite laminates, Composites part A: applied science and manufacturing, 31(10), 2000, 1047-1060. https://doi.org/10.1016/S1359-835X(00)00063-4

[65] United States Government Accountability: Status of FAA's actions to oversee the safety of composite airplanes, AVIATION SAFETY, 2011.

[66] Van Tooren, M.; Jahangir, I.; Elham, A.: Optimization of variable stiffness composite plates with cut-outs subjected to compression, tension and shear using an adjoint formulation, 57th AIAA/ASCE/AHS/ASC Structures, Structural Dynamics, and Materials Conference, 2016.

[67] Vaniglia, M.: Washington, DC: U.S. Patent No. 5,022,952, 1991, Juin 11.

[68] Waldhart, C.: Analysis of tow-placed, variable-stiffness laminates, Virginia Polytechnic Institute and State University, 1996.

[69] Wang, X.; Zhang, W.; Zhang, L.: Intersection of a ruled surface with a free-form surface, Numer Algor, 46(1), 2007, 85–100. https://doi.org/10.1007/s11075-007-9118-y

[70] Wehbe, R.; Tatting, B.; Harik, R.; Gurdal, Z.; Halbritter, A.; Wanthal, A.: Tow-Path Based Modeling Of Wrinkling During The Automated Fiber Placement Process, The Composites and Advanced Materials Expo 2017 (CAMX 2017), September 11-14, Florida, United States

[71] Wehbe, R.: Modeling of tow wrinkling in automated fiber placement based on geometrical considerations, Master Thesis, University of South Carolina, Columbia, SC, 2017.

[72] Wu, K.; Gürdal, Z.: Thermal testing of tow-placed, variable stiffness panels, Proceedings of the 42nd AIAA/ASME/ASCE/AHS/ASC structures, structural dynamics and materials (SDM) conference. Seattle, WA, US, 2001. https://doi.org/10.2514/6.2001-1190

[73] Wu, K.; Gürdal, Z.; Starne, J.: Structural response of compression-loaded, tow-placed, variable stiffness panels, Proceedings of the 43rd AIAA/ASME/AHS/ASC Structures, Structural Dynamics and Materials Conference, AIAA. Denver, CO, USA, 2002. https://doi.org/10.2514/6.2002-1512

[74] Wu, K.; Tatting, B.; Smith, B.; Stevens, R.; Occhipinti, G.; Swift, J.; . . . Thornburgh, R.: Design and manufacturing of tow-steered composite shells using fiber placement, Proceedings of the 50th AIAA/ASME/ASCE/AHS/ASC Structures, Structural Dynamics and Materials Conference, 2009.

[75] Wu, Z.; Weaver, P.; Raju, G.; Kim, B.: Buckling analysis and optimisation of variable angle tow composite plates, Thin-walled structures, 60, 2012, 163-172. https://doi.org/10.1016/j.tws.2012.07.008

[76] Xia, K.; Harik, R.; Herrera, J.; Patel, J.; Grimsley, B.: Numerical simulation of AFP nip point temperature prediction for complex geometries, Submission to SAMPE 2018 Conference & Exhibition, Long Beach, California, US, 21 – 24 May 2018.

[77] Yan, L.; Chen, Z.; Shi, Y.; Mo, R.: An accurate approach to roller path generation for robotic fibre placement of free form surface composites, Robotics and Computer-Integrated Manufacturing, 30(3), 2014, 277-286. https://doi.org/10.1016/j.rcim.2013.10.007

[78] Zamani, Z.; Haddadpour, H.; Ghazavi, M. R.: Curvilinear fiber optimization tools for design thin walled beams, Thin-Walled Structures, 49(3), 2011, 448–454. https://doi.org/10.1016/j.tws.2010.08.002

[79] Zhu, Y.; Liu, J.; Liu, D.; Xu, H.; Yan, C.; Huang, B.; Hui, D.: Fiber path optimization based on a family of curves in composite laminate with a center hole, Composites Part B: Engineering, 111, 2017, 91-102. https://doi.org/10.1016/j.compositesb.2016.11.051

8 APPENDIX

The first fundamental coefficient of the surface $S(u,v)$ are given by:

$$E(u,v) = S_u \cdot S_u \ , \ \ F(u,v) = S_u \cdot S_v, \text{ and } \ G(u,v) = S_v \cdot S_v \tag{8.1}$$

where the symbol "$\cdot$" denotes the dot product, and the subscripts represent the partial derivative with respect to the corresponding variable.

The Christoffel symbols of the surface S are given by:

$$
\begin{aligned}
\Gamma_{11}^1 &= \frac{G\,E_u - 2\,F\,F_u + F\,E_v}{2(E\,G - F^2)} \ , \quad \Gamma_{11}^2 = \frac{2\,E\,F_u - E\,E_v - F\,E_u}{2(E\,G - F^2)} \\
\Gamma_{12}^1 &= \frac{G\,E_v - F\,G_u}{2(E\,G - F^2)} \quad , \quad \Gamma_{12}^2 = \frac{E\,G_u - F\,E_v}{2(E\,G - F^2)} \\
\Gamma_{22}^1 &= \frac{2\,G\,F_v - G\,G_u - F\,G_v}{2(E\,G - F^2)} \ , \quad \Gamma_{22}^2 = \frac{E\,G_v - 2\,F\,F_v + F\,G_u}{2(E\,G - F^2)}
\end{aligned}
\tag{8.2}
$$